Boundary criticality and multifractality at the two-dimensional spin quantum Hall transition

Arvind R. Subramaniam and Ilya A. Gruzberg
Department of Physics and James Franck Institute, University of Chicago, 5640 S. Ellis Avenue, Chicago, Illinois 60637, USA

Andreas W. W. Ludwig
Department of Physics, University of California–Santa Barbara, Santa Barbara, California 93106, USA
(Received 9 May 2008; published 5 December 2008)

Multifractal scaling of critical wave functions at a disorder-driven (Anderson) localization transition is modified near boundaries of a sample. Here this effect is studied for the example of the spin quantum Hall plateau transition using the supersymmetry technique for disorder averaging. Upon mapping the spin quantum Hall transition to the classical percolation problem with reflecting boundaries, a number of multifractal exponents governing wave-function scaling near a boundary are obtained exactly. Moreover, additional exact boundary scaling exponents of the localization problem are extracted, and the problem is analyzed in other geometries.

DOI: 10.1103/PhysRevB.78.245105 PACS number(s): 73.20.Fz, 72.15.Rn, 73.43.−f

I. INTRODUCTION

In a system of noninteracting electrons, disorder can induce transitions between metallic (delocalized) and insulating (localized) phases.[1] The scaling theory of localization[2] predicts that in two dimensions, all single-particle electronic states are typically localized by arbitrarily weak disorder. Consequently, there are no metal-insulator transitions for noninteracting electrons (except in the situations discussed below). This scaling idea can be substantiated quantitatively through a nonlinear-sigma-model (NLSM) formulation of the problem using either the replica[3] or supersymmetry[4] method. The NLSM approach has been very successful in providing a quantitative understanding of the metal-insulator critical point in dimensions greater than two (for a review, see Refs. 5 and 6).

There are two well-known exceptions to the above discussion. One is the two-dimensional (2D) integer quantum Hall (IQH) plateau transition and the other is the metal-insulator transition in 2D systems with spin-orbit scattering (the so-called symplectic symmetry class). These possess phases of both localized and extended states in two dimensions. On one hand, both these transitions can be formulated as NLSM field theories[7,8] (containing an additional topological term in the IQH case). But, on the other hand, these field theories cannot be used to perform analytical (or even perturbative) calculations of critical exponents or other (universal) physical quantities at the transition. This is because the long-distance physics relevant for the properties at the transition is governed by the strong-coupling regime of these theories, which is in general not tractable. Indeed, such a calculation would require a nonperturbative approach to these problems. Some progress on these types of problems has been possible in recent years due to the appearance of models which are analytically tractable even at strong coupling and which exhibit similar localization-delocalization (LD) transitions, but belong to symmetry (and universality) classes different from the ones discussed above. Indeed, seminal work due to Zirnbauer[9] and Altland and Zirnbauer,[10] which appeared a little more than a decade ago, identified a total of ten symmetry classes, describing in principle all possible behaviors of noninteracting quantum-mechanical particles subject to random disorder potentials. Examples of such analytically tractable 2D LD transitions include 2D Dirac fermions subject to random Abelian[11] and non-Abelian gauge potentials,[12,13] the spin quantum Hall (SQH) plateau transition[14–17] (reviewed briefly in Sec. II), and problems with a special so-called sublattice symmetry.[18]

LD transitions are different in several respects from continuous phase transitions occurring in nonrandom systems, such as the ordering transition in a clean ferromagnet. One difference is the absence of an obvious order parameter in many cases. The disorder-averaged density of states, which would be expected to play the role of an order parameter, is not critical[3] at many conventional LD transitions, including those mentioned at the beginning of this section. Another very important difference is that the wave functions at the transition exhibit what is known as multifractal-scaling behavior.[6,19–21] This means that the disorder average of the qth power of the (square of) the critical wave-function amplitude scales with the system size L with a nontrivial exponent that has a nonlinear dependence on the power q. In field-theoretic language, multifractality can be understood as the existence of a certain infinite set of fields in the theory which exhibit infinitely many independent anomalous dimensions with certain very special ("convexity") properties.[22] In contrast, analogous infinite sets of fields cannot exist in "conventional," nonrandom phase transitions. (In two dimensions, for example, such clean phase transitions are known to possess only a finite number of independent anomalous dimensions.[23]) On one hand, the multifractal-scaling properties of wave functions at the 2D IQH plateau transition and at the 2D symplectic class metal-insulator transition have been calculated numerically to high precision.[24–26] On the other hand, the entire multifractal spectrum has been obtained analytically for Dirac fermions in random gauge potentials,[11,13,27,28] while the first few multifractal wave-function moments have been calculated analytically for the spin quantum Hall transition.[29,30]

The aforementioned properties, while being important characteristics of the LD critical points, do not exhaust all their important universal physics. It is well known that even

for nonrandom, conventional phase transitions, the geometry of the system has a crucial effect on the critical behavior.[31] Critical exponents as well as correlation functions depend on the overall geometry and the location where these quantities are measured. In particular, correlation functions of quantities located near the boundary of the system exhibit in general a different scaling behavior[32–34] as compared to bulk correlation functions (and this depends in general also on the imposed boundary conditions). These aspects can be studied in great detail especially in the case of critical 2D systems which are conformally invariant.[35] These ideas thus emphasize the importance of boundary effects in LD transitions, particularly in two dimensions where these transitions are believed to be in general described by conformally invariant fixed points (see also Ref. 26). The SQH transition, being analytically tractable, provides us with a playground where we can understand the effect of both multifractality and boundary criticality at LD transitions. In the process we are led to a more general framework where one considers multifractal behavior of wave functions near boundaries, giving rise to the notion of "surface (boundary) multifractality." The power of conformal invariance enables us to extend this idea to more complicated geometrical settings. In the present paper we derive several exact exponents characterizing these properties for the SQH transition.

To summarize our main results, we note that within a second-quantized formulation of the conventional Chalker-Coddington network model for the SQH transition,[15,17] a reflecting boundary (where the system simply ends) preserves the full sl(2|1) supersymmmetry present in the disorder-averaged bulk problem. After the mapping[17] to bond percolation, this amounts to a reflecting boundary condition for the perimeters (hulls) of the percolation clusters. Here we express correlation functions characterizing wave-function multifractality in terms of the generators of the underlying sl(2|1) supersymmmetry algebra. Using the representation theory of this superalgebra together with the percolation mapping, we are able to convert the correlation functions to classical percolation probabilities. Using previously known scaling exponents for percolation, we are able to calculate two nontrivial multifractal exponents, conventionally denoted by Δ_2 and Δ_3, both on the boundary and in the bulk, within the supersymmetry approach developed in Ref. 17. (The values for Δ_2 and Δ_3 *in the bulk* were obtained in Refs. 29 and 30 using methods very different from the supersymmetry methods used in the present paper.) The inability to calculate higher multifractal moments is explained within our (supersymmetry) formulation. The scaling exponents of the averaged local density of states and point-contact conductance are also found at the boundary. Using suitable conformal invariance arguments, we are able to translate the boundary ("surface") exponents to a wedge geometry and find the corresponding corner exponents. (See Sec. VI for the various exact values.)

The organization of this paper is as follows. In Sec. II we briefly present the physics of the SQH effect. In Sec. III, we discuss the supersymmetry (SUSY) formulation of the Chalker-Coddington network model for the SQH transition in the presence of boundaries. In Sec. IV, we elucidate how supersymmetry in the SQH problem can be used to study (low-order) multifractal wave-function moments, both near boundaries and in the bulk. (As mentioned above, exponents of low-order multifractal moments in the bulk were obtained previously in Ref. 30 using very different methods.) We also explain, using the supersymmetry approach and following Ref. 17, the technical reasons why this computation can be done only for low multifractal moments (up to the third power of the wave-function intensity) and not for the whole multifractal spectrum. The reasons appear to be different from and complementary to the ones discussed in Ref. 30. In Sec. V we discuss the scaling behavior of the local density of states and of the point-contact conductance near a boundary. In Sec. VI, we extend our discussion to more complicated geometries. In Sec. VII, we conclude by discussing certain implications of our results and a number of remaining open issues. Some of the results derived in the present paper were announced in Ref. 36.

II. PHYSICS OF THE SPIN QUANTUM HALL TRANSITION

The SQH transition was first studied, numerically, in Ref. 15. A simple physical picture of the SQH effect was given in Ref. 16. In this section we briefly review, for completeness, the basic physics of the SQH effect.

Let us consider a lattice version of the Bogoliubov-de Gennes (BdG) Hamiltonian describing a singlet superconductor (classes C or CI in the notation of Refs. 9 and 10):

$$\mathcal{H} = \sum_{ij} \left(t_{ij} \sum_{\alpha} c_{i\alpha}^{\dagger} c_{j\alpha} + \Delta_{ij} c_{i\uparrow}^{\dagger} c_{j\downarrow}^{\dagger} + \Delta_{ij}^{*} c_{j\downarrow} c_{i\uparrow} \right). \tag{1}$$

The first term here describes (in a second-quantized language) hopping of electrons of either spin $\alpha = \uparrow, \downarrow$ between lattice sites i and j, as well as possible on-site potentials (for $i=j$). The other two terms describe BCS singlet pairing. Provided that the gap function satisfies $\Delta_{ij} = \Delta_{ji}$, Hamiltonian (1) is SU(2) invariant and commutes with the three generators of the global SU(2) spin rotations (total spin):

$$\vec{S} = \frac{\hbar}{2} \sum_{i} c_{i\alpha}^{\dagger} \vec{\sigma}_{\alpha\beta} c_{i\beta}. \tag{2}$$

The BdG Hamiltonian (1) does not conserve the particle number or charge. Physically this is due to the existence of the pair condensate which may exchange electrons into holes in processes similar to Andreev reflection. Not being a conserved quantum number, the quasiparticle charge cannot be transported by diffusion. Consequently, there is no notion of electrical (charge) conductivity. However, the spin of each quasiparticle is conserved by Hamiltonian (1). One may define the spin conductivity as the linear-response coefficient between the (say) z component of the spin current and the gradient of a Zeeman field along the z direction:

$$j_i^z = -\sigma_{ij}^s g \mu_B \partial_j B^z. \tag{3}$$

Here g is the gyromagnetic ratio, and μ_B is the Bohr magneton.

When the gap function Δ is complex, time-reversal symmetry is broken, and then the Hall (transverse) spin conduc-

tivity σ^s_{xy} may be nonvanishing. It is convenient to perform a particle-hole transformation on the down-spin particles:

$$d_{i\uparrow} = c_{i\uparrow}, \quad d_{i\downarrow} = c^\dagger_{i\downarrow}. \tag{4}$$

Under this transformation the z component of the generator of spin rotations in Eq. (2) becomes simply the total number of d particles, $\frac{\hbar}{2}\Sigma_{i,\alpha} d^\dagger_{i\alpha} d_{i\alpha}$. Thus the transformation interchanges the role of particle number and z component of spin, with the result that the transformed Hamiltonian conserves the number of d particles:

$$\mathcal{H} = \sum_{ij} d^\dagger_{i\alpha} H_{ij,\alpha\beta} d_{j\beta}. \tag{5}$$

Here H_{ij} is the so-called Bogoliubov–de Gennes (BdG) Hamiltonian, a 2×2 matrix in the spin space:

$$H_{ij} = \begin{pmatrix} t_{ij} & \Delta_{ij} \\ \Delta^*_{ij} & -t^*_{ij} \end{pmatrix}. \tag{6}$$

Since the d-particle number is conserved, we can use a single-particle description. The external nonrandom Zeeman field B^z in the z direction in this alternative description maps onto a simple shift ϵ in the Fermi energy as

$$\epsilon = g\mu_B B^z. \tag{7}$$

The spin conductivity in the original problem becomes the usual electrical (charge) conductivity of the d particles. Note that the role of the elementary charge is now played by $\hbar/2$, so that the natural quantum of the spin conductivity is $(\hbar/2)^2/2\pi\hbar = \hbar/8\pi$. In what follows we use units in which $\hbar = 1$.

Invariance of the Hamiltonian in Eq. (1) under the global SU(2) symmetry implies the following property of the matrix H_{ij} in Eq. (6):

$$\sigma_y H_{ij} \sigma_y = -H^*_{ij}, \tag{8}$$

which has important consequences. First, it implies that the eigenvalues of H_{ij} always appear in pairs as $(\epsilon, -\epsilon)$. In other words, the single-particle energy spectrum is symmetric about $\epsilon = 0$. The ground state of the problem is obtained by filling up all the negative-energy (d) single-particle states. The positive-energy (d) particle and hole excitations on top of this ground state are doublets under the global SU(2) symmetry. A Zeeman term, or non-zero energy-shift [see Eq. (7)], breaks the global SU(2) symmetry and splits the degeneracy between the above-mentioned (d) particle and hole states. Second, Eq. (8) implies a relation between the retarded and advanced Green's functions of the BdG Hamiltonian or the corresponding network model (see Eq. (16)].

A clean (that is, nonrandom) $d_{x^2-y^2}+id_{xy}$-wave superconductor (which breaks time-reversal symmetry) can, for example, be obtained on the lattice with a gap function Δ_{ij} whose Fourier transform is (square lattice "d-wave")

$$\Delta_k = \Delta_0(\cos k_x - \cos k_y) - i\Delta_{xy} \sin k_x \sin k_y. \tag{9}$$

It is easy to see[16] that this represents at low energies a (2+1)-dimensional Dirac fermion of mass Δ_{xy}, leading[11] to a quantized spin Hall conductivity (in units of $\hbar/8\pi$):

$$\sigma^s_{xy} = 2 \text{ sgn } \Delta_{xy}. \tag{10}$$

This is consistent with the existence of two spin-current-carrying states at the edge of a system with a boundary (say, to vacuum).

These edge states, being chiral, survive the addition of weak disorder, so the quantization of σ^s_{xy} persists in a disordered d-wave superconductor with broken time-reversal invariance, at least for weak disorder. In general, there can be two possible localized phases—spin insulator and SQH phase—distinguished topologically by the quantized value of the spin Hall conductivity. A transition between them, the generic SQH transition, is a localization-delocalization transition similar to the IQH plateau transition, where σ^s_{xy} jumps by two units. It is a quantum-percolation transition[37] of the edge states forming[11] at the interfaces between two topologically distinct regions.

There is one essential difference between the SQH and the IQH cases. In the latter case, the mean single-particle density of states is nonvanishing on either side and at the transition. In the SQH case, on the other hand, the density of states of d particles, $\rho(\epsilon)$, vanishes at zero energy, $\epsilon = 0$, in both localized phases[38] as ϵ^2. Right at the transition, that is, at $\epsilon = 0$, it vanishes (as might have been expected) with a nontrivial exponent:

$$\rho(\epsilon) \sim |\epsilon|^\alpha. \tag{11}$$

The exponent α was calculated exactly in Ref. 17 to be 1/7. In Sec. V below we will present a derivation of this result, as well as its analog for the local density of states at a boundary of the SQH system.

III. SQH NETWORK MODEL

A. Description of the network

Network models have been very convenient for both numerical and analytical work on various disordered noninteracting-fermion problems. The best known such model is the Chalker-Coddington (CC) network model[39] for the integer quantum Hall plateau transition. Similar network models can be constructed for other localization problems, including the chiral metal,[40,41] the SQH transition,[15–17] the random bond Ising model, and the thermal quantum Hall effect.[42–45]

The SQH network consists of a lattice of directed links and two types of nodes, A and B, forming a square lattice (see Fig. 1) on which spin-1/2 particles at energy $\epsilon = 0$ can propagate. Unidirectional propagation through each link is represented by a random SU(2) matrix. As in the case of CC network, to study the critical behavior at the SQH transition it is sufficient to introduce disorder only for propagation along the links, while all the nodes can be taken to have the same (nonrandom) scattering matrices. The node scattering matrices are diagonal in the spin indices: $S_S = S_{S\uparrow} \otimes S_{S\downarrow}$,

$$S_{S\sigma} = \begin{pmatrix} (1-t^2_{S\sigma})^{1/2} & t_{S\sigma} \\ -t_{S\sigma} & (1-t^2_{S\sigma})^{1/2} \end{pmatrix}, \tag{12}$$

where $S = A, B$ labels whether the node is on the A or the B sublattice, and $\sigma = \uparrow, \downarrow$ labels the spin index of the propagat-

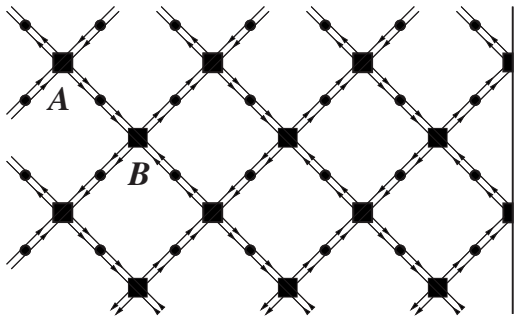

FIG. 1. SQH network with a vertical reflecting boundary. The black squares represent the nonrandom node scattering matrices [Eq. (12)]. The black circles on the links represent the random SU(2) scattering matrices.

ing particle. Apart from the case of boundary nodes (which will be treated in detail later), the remaining network is isotropic (invariant under 90° rotation of the lattice) when the scattering amplitudes on the two sublattice nodes are related by $t_{A\sigma}^2+t_{B\sigma}^2=1$. The critical point of the isotropic network is located at $t_{A\sigma}=t_{B\sigma}=1/\sqrt{2}$. Varying $t_{S\sigma}$ while keeping $t_{A\sigma}^2+t_{B\sigma}^2=1$ and $t_{S\uparrow}=t_{S\downarrow}$ drives the system between a spin insulator and a SQH state and the spin Hall conductance jumps from 0 to 2. Taking $t_{S\uparrow}\neq t_{S\downarrow}$ breaks the global SU(2) symmetry and splits the transition into two ordinary IQH transitions each in the unitary symmetry class (investigated, for example, in Ref. 39). In this paper we consider only the spin-rotation-invariant case with $t_{S\uparrow}=t_{S\downarrow}=t_S$.

B. Green's functions and symmetries

Network models can be studied using either a first-quantized or a second-quantized formalism. The first-quantized method is adopted in Refs. 30 and 46. It is also very useful for numerical work. Here we use it to derive certain symmetry relations. The rest of the paper will employ the second-quantized formalism (see Sec. III C).

All physical quantities of interest in our problem such as wave-function correlators and conductance can be expressed in terms of the Green's functions. Usually, the latter are represented in continuous-time notation, but the network models use the discrete-time analogs. In particular, network models use a single-step time-evolution operator $\mathcal{U}$ which acts on the single-particle wave function $\Psi(r,t)$ at discrete time t to give the wave function at time $t+1$, where r denotes a link of the network. For a network with N links, $\mathcal{U}$ is (due to the spin index) a $2N\times 2N$ matrix, which represents a finite-time version of the infinitesimal time-evolution operator. Thus $\mathcal{U}=\exp\{i\mathcal{H}\}$, where the Hamiltonian $\mathcal{H}$ (which describes the time evolution of the edge states separating "puddles" of topologically distinct regions) has the same symmetry properties as the underlying BdG Hamiltonian in Eq. (6). Therefore, due to the property in Eq. (8), $\mathcal{U}$ is a (unitary) symplectic matrix and as such satisfies the condition

$$\mathcal{U}^{-1}=\sigma_y\mathcal{U}^T\sigma_y, \tag{13}$$

where σ_y is the conventional Pauli matrix.

Now we can write the retarded (advanced) Green's function $G_R(r_1,r_2)$ $[G_A(r_1,r_2)]$ as the resolvent of the operator $\mathcal{U}$:

$$[G_R(r_1,r_2)]_{\alpha\beta}=\langle r_1,\alpha|\frac{1}{1-z\mathcal{U}}|r_2,\beta\rangle, \tag{14}$$

$$[G_A(r_1,r_2)]_{\alpha\beta}=\langle r_1,\alpha|\frac{1}{1-z^{-1}\mathcal{U}}|r_2,\beta\rangle. \tag{15}$$

Here $z=e^{i(\epsilon+i\gamma)}$, where ϵ is the energy and γ is a finite level broadening. Since the SQH transition of interest to us occurs only at zero energy, we will set $\epsilon=0$ and hence $z=e^{-\gamma}$ from here on. In the above equation, r_1 and r_2 and α and β denote the network link and the spin index, respectively.

Making use of Eq. (13) in Eqs. (14) and (15) leads to the following relationship between the advanced and retarded Green's functions:

$$[G_A(r_1,r_2)]_{\alpha'\alpha}-\delta_{\alpha'\alpha}\delta_{r_1,r_2}=\epsilon_{\alpha\beta}[G_R(r_2,r_1)]_{\beta\beta'}\epsilon_{\beta'\alpha'}, \tag{16}$$

where $\epsilon_{\alpha\beta}$ is the antisymmetric Levi-Civitá tensor. The above equation will turn out to be crucial for our calculations since it implies that we need not introduce separate operators for the advanced sector Green's functions but can work solely with retarded ones (as we will see below).

C. Second-quantized description in the bulk

All network models can also be studied using the second-quantized SUSY technique.[41,47] The second quantization of the SQH network is described in Ref. 17 and we review the main steps here. The basic idea is quite similar to the transfer matrix formulation of various 2D statistical-mechanics problems such as the Ising model (for a review, see Ref. 48). The presence of disorder introduces a number of additional features which are sketched below.

All physical quantities in the network model including conductance and wave-function amplitudes may be expressed in first quantization in terms of sums over paths on the network. Such a sum may be written in second-quantized SUSY language as a correlation function, $\langle\cdots\rangle\equiv\mathrm{STr}[\cdots(U_BU_A)^{L_T}]$, where the supertrace "STr" contains the row-to-row transfer matrices U_A and U_B and the ellipsis $\cdots$ stands for operators that are inserted at the beginning and the ends of paths and correspond physically to density, current, etc. L_T is the number of A nodes (or B nodes) along the vertical direction, interpreted as discrete (imaginary) time. [The operator $(U_BU_A)^{L_T}$ was denoted by U in Ref. 17.] The supertrace STr implements periodic boundary condition along the vertical direction. Let there be L_X nodes in each row (the "horizontal" or X direction). The operator U_A (U_B) is formed by multiplying all the L_X transfer matrices at A (B) nodes in a given row. These matrices act on a tensor product of bosonic and fermionic Fock spaces defined for each vertical column of links. The quantum state in the Fock spaces in each horizontal row of links should be thought of as resulting from the quantum state of the previous (in discrete imaginary time) row upon action of either U_A or U_B, within a single time step. The presence of a fermion or boson

on a link represents an element of a path traversing that link.[41,47] Both bosons and fermions are needed to ensure the cancellation of contributions from closed loops [this ensures that $\mathrm{STr}(U_B U_A)^{L_T}=1$].

Usually one needs two types of bosons and fermions, "retarded" and "advanced," to be able to obtain two-particle properties (that is, averages of products of retarded and advanced Green's functions) relevant for the calculation of transport properties. However, the symmetry relation in Eq. (16) relates retarded and advanced Green's functions. Hence, as it turns out, for the computation of low enough moments of, say, retarded Green's functions, we need only one fermion and one boson per spin direction per link of a row. (This will be discussed in detail below.) We denote them by f_σ and b_σ for the links going up (up links) and $\bar{f}_\sigma$ and $\bar{b}_\sigma$ for the down links. On the up links, f_σ and b_σ satisfy canonical fermion anti-commutation and boson commutation relations, respectively. But to ensure the cancellation of closed loops, we must either take the fermions on the down links to satisfy the modified anti-commutation relations: $\{\bar{f}_\sigma, \bar{f}^\dagger_{\sigma'}\}=-\delta_{\sigma\sigma'}$ (while the bosons on the down links, b_σ and $b^\dagger_\sigma$ satisfy the canonical commutation relations), or, alternatively, we take the bosons on the down links to satisfy the modified commutation relations: $[\bar{b}_\sigma, \bar{b}^\dagger_{\sigma'}]=-\delta_{\sigma\sigma'}$ (while the fermions on the down links, f_σ and $f^\dagger_\sigma$satisfy the canonical anti-commutation relations). Each node transfer matrix can be written in terms of these bosons and fermions. For any given disorder realization, this node transfer matrix turns out to commute with all the generators of the sl(2|1) superalgebra, as shown in Ref. 17 (see appendix A for a summary of the relevant superalgebra representation theory). Performing the average over disorder (independently on each link) projects[17] the Fock space of bosons and fermions into the fundamental (dual-fundamental) three-dimensional representation of sl(2|1) on up links (down links). These are precisely the states which are singlets under the random ("gauge") SU(2) on the links.

D. Network boundary

The extension of the above formalism to the case of a network with a reflecting boundary in the vertical direction is straightforward. Relegating some technical details to Appendix B, the reflecting boundary is seen to preserve the full sl(2|1) SUSY present in the bulk. Using the fully intact supersymmetry, one can then retain the mapping to the perimeters of percolation clusters (we refer to them as hulls henceforth) obtained in Ref. 17, but now the percolation hulls are confined to the half plane in two dimensions with a reflecting boundary (see Fig. 1).

We will consider below correlation functions of operators in the network model in the vicinity of the SQH transition. When using continuum notation one needs to recall[32–34] that, in general, operators acquire additional singularities when approaching a boundary; they may vanish or diverge. By saying that points lie on the boundary, we imply that these points are not literally located *at* the boundary, but rather that the distance of the points from the boundary is much smaller than the distance of these points from each other, and much smaller than the system size. The same general reasoning will apply when we consider multifractality of wave functions at the boundary. Let us recall that in the literature of surface transitions in ordinary magnets, various kinds of cases which are often referred to as "ordinary," "extraordinary," and "special" boundary transitions are discussed, referring to the respective ordering of bulk and boundary. The case of the reflecting boundary condition that we consider here is analogous to the so-called ordinary surface transition where the boundary and the bulk undergo the LD transition simultaneously.

We will need the bulk and boundary scaling dimensions of the one-hull operator of critical percolation in various calculations below. This has been derived using a variety of techniques in the literature[35,49,50] and is found to be $x_s=1/3$ for the boundary one-hull operator. The corresponding bulk operator has scaling dimension $x_b=1/4$.

IV. MULTIFRACTALITY USING SUPERSYMMETRY

A. Wave-function correlators

In the context of LD transitions, multifractality manifests itself through the anomalous scaling with system size of the moments of the square of the wave-function amplitude, $|\psi(r)|^2$ (wave-function "intensity"), at criticality (see, for example, Refs. 6 and 20). The wave-function moments conventionally appear in the form of the so-called averaged generalized inverse participation ratios (IPRs) P_q (the overbar denotes disorder average),

$$P_q = \int_{\mathcal{M}_x} d^{D_x} r_x \overline{|\psi(r_x)|^{2q}} \propto L^{D_x} \overline{|\psi(r_x)|^{2q}}, \tag{17}$$

whose scaling with linear system size L at a critical point defines the critical exponents τ^x_q and Δ^x_q (often referred to as "anomalous dimension"),

$$P_q \propto L^{-\tau^x_q}, \quad \tau^x_q = dq + \Delta^x_q + q\mu_x - D_x. \tag{18}$$

Here, D_x is the dimension of the region $\mathcal{M}_x$ over which the integration is performed in Eq. (17). In particular, we will be interested in the cases of bulk ($x=b$), boundary ($x=s$), and corner ($x=c$) where D_x takes on, respectively, the values d, $d-1$, and $d-2$. The corresponding anomalous dimensions will be denoted by Δ^b_q, Δ^s_q, and Δ^c_q. One notes that $\Delta^b_1=0$ due to the fact that wave functions are normalized to unity with respect to the whole system (implying $P_{q=1}=1$ and $\mu_b=0$). There is no such general constraint for Δ^s_1 and Δ^c_1. However, we adopt the convention of setting them equal to zero and the corresponding contribution to τ^x_1 is reflected in μ_s and μ_c, respectively. With this choice, a nonvanishing exponent μ_x characterizes a nontrivial scaling behavior of the local wave-function intensity at the sample location r_x,

$$L^d \overline{|\psi(r_x)|^2} \propto 1/L^{\mu_x}, \tag{19}$$

which is known to occur in certain nonconventional Anderson-localization symmetry classes,[9,10] as was discussed previously in Ref. 36.

The wave-function moments have a natural interpretation as operators in a field theory describing the LD transition. As

an aside, it is worthwhile emphasizing that the interpretation of multifractal moments in terms of field-theory operators is a very general one and not just restricted to LD transitions (see Ref. 22 for a discussion of this point). We have defined multifractal exponents in terms of moments of wave function at a single point in the sample in Eq. (17). In field theory, for calculating the multifractal exponent Δ_q^x (restricting q to be an integer), it is easier to find the scaling of correlation function of q operators, each corresponding to the wave-function intensity $L^2|\psi(r)|^2$. The q-point correlations of critical eigenfunction intensities take on a convenient scaling form when the distances between all points are equal to the same scale r, that is, $|r_i - r_j| \sim r$, and it follows that

$$L^{q(d+\mu_x)}\overline{|\psi(r_1)\psi(r_2)\cdots\psi(r_q)|^2} \sim \left(\frac{r}{L}\right)^{\Delta_q^x}, \tag{20}$$

where L is the linear system size.

Off criticality (that is, for $\epsilon \neq 0$ or $\gamma > 0$ in the SQH system), multifractal-scaling behavior holds on length scales much shorter than the localization length[17] $\xi_\gamma \sim \gamma^{-4/7}$, beyond which the wave-function amplitudes are exponentially small.[29,30] This implies that off criticality, the above q-point correlator should be written as

$$L^{q(d+\mu_x)}\overline{|\psi(r_1)\psi(r_2)\cdots\psi(r_q)|^2} \sim \left(\frac{r}{\xi_\gamma}\right)^{\Delta_q^x}, \quad r \ll \xi_\gamma. \tag{21}$$

Assuming that all wave functions at a given energy show statistically identical multifractal-scaling behavior, one can write the left-hand side (LHS) of the above correlator as

$$L^{q(d+\mu_x)}\overline{|\psi(r_1)\psi(r_2)\cdots\psi(r_q)|^2} = \frac{\overline{\sum_{i_1,i_2,\ldots,i_q} |\psi_{i_1}(r_1)\psi_{i_2}(r_2)\cdots\psi_{i_q}(r_q)|^2 \delta(\epsilon_1-\epsilon_{i_1})\delta(\epsilon_2-\epsilon_{i_2})\cdots\delta(\epsilon_q-\epsilon_{i_q})}}{\overline{\rho(\epsilon_1)\rho(\epsilon_2)}\cdots\overline{\rho(\epsilon_q)}}, \tag{22}$$

where $i_1, i_2, \ldots, i_q$ are additional quantum numbers required, besides position r, to label the wave function (energy and spin in the SQH case). ρ represents the global density of states. Taking $\epsilon_1, \epsilon_2, \ldots, \epsilon_q \sim \epsilon$ and $|r_i - r_j| \sim r$, we see that the exponent Δ_q^x is given by the scaling behavior of $\tilde{\mathcal{D}}_q^x(r_1, r_2, \ldots, r_q; \epsilon)$ with respect to r, where the function $\tilde{\mathcal{D}}_q^x$ is defined by

$$\tilde{\mathcal{D}}_q^x(r_1, r_2, \ldots, r_q; \epsilon) = \overline{\sum_{i_1,i_2,\ldots,i_q} |\psi_{i_1}(r_1)\psi_{i_2}(r_2)\cdots\psi_{i_q}(r_q)|^2 \delta(\epsilon-\epsilon_{i_1})\delta(\epsilon-\epsilon_{i_2})\cdots\delta(\epsilon-\epsilon_{i_q})}. \tag{23}$$

We understand that the points $r_1, \ldots, r_q$ are all chosen to lie in the region $\mathcal{M}_x$ considered in Eq. (17).

Using the Green's functions defined in Sec. III B, we can write the above wave-function correlator as [ignoring overall factors of $(2\pi)^{-q}$] as

$$\tilde{\mathcal{D}}_q^x(r_1, r_2, \ldots, r_q; z) \propto \overline{\prod_{k=1}^{q} \mathrm{tr}[G_R(r_k, r_k) - G_A(r_k, r_k)]}. \tag{24}$$

Here "tr" denotes the trace over the spin indices. As was discussed in Ref. 30, the multifractal exponents can also be obtained from a different Green's-function product,

$$\mathcal{D}_q^x(r_1, r_2, \ldots, r_q; z) \propto \overline{\mathrm{tr} \prod_{k=1}^{q} [G_R(r_k, r_{k+1}) - G_A(r_k, r_{k+1})]}, \tag{25}$$

where $r_{q+1} \equiv r_1$. When $|r_i - r_j| \sim r$, this product shows the same scaling behavior, $r^{-\Delta_q^x}$, as the previous one. Since the calculations of both functions $\tilde{\mathcal{D}}$ and $\mathcal{D}$ are very similar, we have explained in detail only the calculation of $\tilde{\mathcal{D}}$. By suitably choosing the correct SU(2) invariant (see, for example, Sec. IV B), we will extract below the scaling of $\tilde{\mathcal{D}}$. Our results agree with those previously obtained in Ref. 30 for the *bulk* case, $x=b$, but we obtain these results using a different method (namely, that developed in Ref. 17, using supersymmetry). Our results for the boundary $x=s$ and corner $x=c$ cases have not been obtained before.

B. Calculation of Δ_2^x

We start with the calculation of the exponent Δ_q^x for the case $q=2$. The corresponding Green's-function product that we have to evaluate is [dependence on $z=\exp(-\gamma)$, defined in Eqs. (14) and (15), is understood]

$$\tilde{\mathcal{D}}_2^x(r_1, r_2) \propto \overline{\mathrm{tr}[G_R(r_1, r_1) - G_A(r_1, r_1)]\mathrm{tr}[G_R(r_2, r_2) - G_A(r_2, r_2)]}. \tag{26}$$

Using Eq. (16), we can write the above relation in terms of retarded functions alone as

$$\begin{aligned}\tilde{\mathcal{D}}_2^x(r_1, r_2) &\propto \overline{\mathrm{tr}[G_R(r_1, r_1) - 1]\mathrm{tr}[G_R(r_2, r_2) - 1]} \\ &= \overline{\mathrm{tr}\, G_R(r_1, r_1)\mathrm{tr}\, G_R(r_2, r_2)} - \overline{\mathrm{tr}\, G_R(r_1, r_1)} \\ &\quad - \overline{\mathrm{tr}\, G_R(r_2, r_2)} + 1.\end{aligned} \tag{27}$$

We will use the supersymmetry technique[4] to implement the disorder average and express[17] all averaged Green's functions using the second-quantized formalism in terms of generators of the sl(2|1) Lie superalgebra. (A summary of certain basic elements of the relevant representation theory of the sl(2|1) superalgebra is presented in Appendix A.)

The retarded Green's functions can be expressed as expectation values of canonical boson and fermion operators. (From here on, all Green's functions are understood as retarded unless they have an explicit subscript *A*.) Specifically, we can write the following Green's functions, in any fixed realization of disorder, as (the subscripts below refer to both the spatial coordinate and the spin index)

$$G_{ij} = \mathrm{STr}[b_i b_j^\dagger (U_B U_A)^{L_T}] = \langle b_i b_j^\dagger \rangle,$$

$$G_{kn} = \mathrm{STr}[f_k f_n^\dagger (U_B U_A)^{L_T}] = \langle f_k f_n^\dagger \rangle, \tag{28}$$

$$G_{ij} G_{kn} = \mathrm{STr}[b_i b_j^\dagger f_k f_n^\dagger (U_B U_A)^{L_T}] = \langle b_i b_j^\dagger f_k f_n^\dagger \rangle. \tag{29}$$

[Here, the fact that $\mathrm{STr}(U_B U_A)^{L_T}=1$ was used.] Let us take $i \to (r_1, \alpha_1)$, $j \to (r_1, \beta_1)$, $k \to (r_2, \alpha_2)$, and $n \to (r_2, \beta_2)$ in the above equations. The LHS of the last equation thus reads $G^{\alpha_1}_{\beta_1}(r_1, r_1) G^{\alpha_2}_{\beta_2}(r_2, r_2)$. After performing the disorder average, only SU(2) singlet combinations are nonvanishing. Hence we contract both sides with the SU(2)-invariant $\delta^{\alpha_1}_{\beta_1}\delta^{\alpha_2}_{\beta_2}$, giving LHS $= \overline{\mathrm{tr}\, G(r_1, r_1)\, \mathrm{tr}\, G(r_2, r_2)}$. The right-hand side (RHS) of Eq. (29) is (we can raise and lower indices trivially since the metric is the unit matrix)

$$\begin{aligned} \mathrm{RHS} &= \delta^{\alpha_1}_{\beta_1}\delta^{\alpha_2}_{\beta_2} \langle b_{\alpha_1}(r_1) b^\dagger_{\beta_1}(r_1) f_{\alpha_2}(r_2) f^\dagger_{\beta_2}(r_2) \rangle \\ &= \langle [2B(r_1) + 1][1 - 2Q_3(r_2)] \rangle. \end{aligned} \tag{30}$$

(The expressions for the generators B and Q_3 of the Lie superalgebra, as reviewed in Appendix A, were used.) Thus the LHS and RHS together imply

$$\overline{\mathrm{tr}\, G(r_1, r_1)\, \mathrm{tr}\, G(r_2, r_2)} = \langle [2B(r_1) + 1][1 - 2Q_3(r_2)] \rangle. \tag{31}$$

Similarly, considering Eq. (28), let $k \to (r_2, \alpha_2)$ and $n \to (r_2, \beta_2)$, giving LHS $= G^{\alpha_2}_{\beta_2}(r_2, r_2)$. To do disorder average, contract with the SU(2)-invariant $\delta^{\beta_2}_{\alpha_2}$, giving LHS $= \overline{\mathrm{tr}\, G(r_2, r_2)}$. The RHS of Eq. (28) gives

$$\mathrm{RHS} = \delta^{\beta_2}_{\alpha_2} \langle f_{\alpha_2}(r_2) f^\dagger_{\beta_2}(r_2) \rangle = \langle 1 - 2Q_3(r_2) \rangle. \tag{32}$$

Hence from LHS and RHS, we obtain

$$\overline{\mathrm{tr}\, G(r_2, r_2)} = \langle 1 - 2Q_3(r_2) \rangle. \tag{33}$$

Now using Eqs. (31) and (33), we can write Eq. (27) as

$$\widetilde{\mathcal{D}}^x_2(r_1, r_2) \propto -\langle B(r_1) Q_3(r_2) \rangle. \tag{34}$$

We will now compute this correlator off criticality, at a finite correlation length ξ_γ, arising from a nonvanishing "broadening" $\gamma > 0$, that is, $z = \exp(-\gamma) < 1$.

The angular brackets in Eq. (34) denote the supertrace STr taken over the *full* Fock space of canonical bosons and fermions on each link of the network before disorder averaging. As explained in Ref. 17, the disorder average projects this Fock space into the fundamental three-dimensional representation of sl(2|1) on the up links and the corresponding dual representation on the down links. To sum only over the three states in this representation, we use the notation "str" [see Eq. (35)]. We note that the state with odd fermion number in both of these representations has negative norm.[17] The prefix "s" in str denotes the fact that these negative norm states contribute to the trace with a negative sign. This is essential to get the correct overall factor of unity for each loop traversed.[17] The action of the node transfer matrix, $T_{S\sigma}$, on the tensor product of the disorder-averaged states on an up link and a neighboring down link can be represented by a linear combination of the only two sl(2|1)-invariant operators in this 3×3 dimensional vector space. These are the identity operator and the projection operator onto the singlet state, with weights $1 - t^2_{S\sigma}$ and $t^2_{S\sigma}$, respectively. These weights can be considered as the classical probability of a state turning left or right at a given node under the action of the node transfer matrix. When we multiply all such node transfer matrices together, the partition function can be represented as a sum over all classical configurations of densely packed loops (the closed classical paths along which the disorder-averaged states propagate) on a square lattice. Each loop gets an overall weight which is the product of the probabilities of turning in a particular direction at each node. The loops can be interpreted (see Ref. 17 for a diagrammatic perspective) as the external perimeters of a cluster percolating along the bonds of a square lattice. This completes the mapping to percolation identified in Ref. 17.

Now, in order to evaluate a disorder-averaged correlator such as the one in Eq. (34), consider the three-dimensional representation on the links (for example, the case where r_1 and r_2 lie on up links) and all calculations are done in this representation. A loop passing through a link corresponds to all three states in the three-dimensional sl(2|1) representation propagating on that link. Away from criticality, we assign a factor of $z^{2(B+Q_3)}$ for each such link since the operator $2(B+Q_3)$ counts the number of states propagating on that link. The product of these factors along a path on the network gives the same power of z that occurs in the Taylor expansion of a matrix element of the Green's function in Eq. (14). After multiplying such factors for all links through which a given loop passes, we also multiply it with the overall weight coming from the classical probability of the loop turning at each node as mentioned in the previous paragraph. Further, if there are operators inserted at specific points on the lattice, the only loops contributing to the correlation function are those which are constrained to pass through these points. Considering the correlator in Eq. (34), there are two different kinds of loop configurations which contribute : (1) a single loop passes through both points r_1 and r_2, and (2) two different loops pass through each of these two points r_1 and r_2. These two terms are the probabilistic versions of the usual connected and disconnected parts of any correlation function. Writing the contribution for each of these types separately and summing over all possible loop configurations together with their respective weights, we write Eq. (34) as

$$4\langle B(r_1)Q_3(r_2)\rangle = \sum_{N_{12},N_{21}} \mathrm{str}\begin{pmatrix}1&0&0\\0&2&0\\0&0&1\end{pmatrix}\begin{pmatrix}1&0&0\\0&z^{2N_{12}}&0\\0&0&z^{2N_{12}}\end{pmatrix}\begin{pmatrix}-1&0&0\\0&0&0\\0&0&1\end{pmatrix}\begin{pmatrix}1&0&0\\0&z^{2N_{21}}&0\\0&0&z^{2N_{21}}\end{pmatrix}P(r_1,r_2;N_{12},N_{21})$$
$$+\sum_{N,N'} \mathrm{str}\begin{pmatrix}1&0&0\\0&2&0\\0&0&1\end{pmatrix}\begin{pmatrix}1&0&0\\0&z^{2N}&0\\0&0&z^{2N}\end{pmatrix}\mathrm{str}\begin{pmatrix}-1&0&0\\0&0&0\\0&0&1\end{pmatrix}\begin{pmatrix}1&0&0\\0&z^{2N'}&0\\0&0&z^{2N'}\end{pmatrix}P_-(r_1,r_2;N,N')$$
$$=-\sum_N [1-z^{2N}]P(r_1,r_2;N)-\sum_{N,N'}[1-z^{2N}][1-z^{2N'}]P_-(r_1,r_2;N,N'), \tag{35}$$

where $P(r_1,r_2;N)$ is the probability of a single loop of length N passing through both r_1 and r_2, and $P_-(r_1,r_2;N,N')$ is the probability that in a given percolation configuration the points r_1 and r_2 belong to two different, nonoverlapping loops of lengths N and N', respectively. In the above equation, the probability factor $P(r_1,r_2;N_{12},N_{21})$ is for a path of length N_{12} going from r_1 to r_2 and then a path of length N_{21} returning from r_2 to r_1. In the next line, we simplified this using the fact that this is the same as a loop of overall length $N=N_{12}+N_{21}$ passing through both the points, and setting $P(r_1,r_2;N) \coloneqq P(r_1,r_2;N_{12},N_{21})$. The appearance of these classical percolation probabilities in the above formula arises from the product of the individual factors for turning left or right at each node of the network model. Thus, using Eq. (35), we can write Eq. (34) as

$$\tilde{\mathcal{D}}_2^x(r_1,r_2) \propto \sum_N [1-z^{2N}]P(r_1,r_2;N) + \sum_{N,N'}[1-z^{2N}][1-z^{2N'}]P_-(r_1,r_2;N,N'). \tag{36}$$

We see that the leading-order terms turn out to vanish in the critical limit $z\to 1$, as observed in Ref. 30. So we need to consider the subleading behavior. The percolation probabilities discussed above are the Laplace-transformed versions of the correlation functions of one-hull operators in percolation. The one-hull operator represents the density-of-states operator in the SQH problem.[17] We know the scaling dimension of these operators as mentioned in the last paragraph in Sec. III D. Under the Laplace transform, the variable N is the conjugate of the energy $\epsilon+i\gamma \equiv -i \ln z$ which is represented by the one-hull operator. Now, using the scaling dimensions of the one-hull operator to deduce the scaling of the Laplace-transformed correlation functions (see, for example, Ref. 51), one finds the following leading scaling behavior of the above-mentioned probabilities:

$$P(r_1,r_2;N) \sim N^{-2/(2-x_b)}r^{-x_b} \sim N^{-8/7}r^{-1/4}, \tag{37}$$

$$P_-(r_1,r_2;N,N') \sim P(r_1;N)P(r_2;N') \sim N^{-8/7}N'^{-8/7}, \tag{38}$$

where $P(r_1;N)$ is the probability that the point r_1 belongs to a loop of length N. The points r_1 and r_2 lie in the bulk and $r=|r_1-r_2| \ll \xi_\gamma \sim \gamma^{-4/7} \sim N^{4/7}$. Similarly, the scaling expressions in the case where both points lie on the boundary are

$$P(r_1,r_2;N) \sim N^{-1-x_s/(2-x_b)}r^{-x_s} \sim N^{-25/21}r^{-1/3}, \tag{39}$$

$$P_-(r_1,r_2;N,N') \sim P(r_1;N)P(r_2;N') \sim N^{-25/21}N'^{-25/21}. \tag{40}$$

We see that only the first term in Eq. (36) (which is the connected part) gives rise to the nonanalytic r dependence in the limit $r \ll \xi_\gamma$, which we are interested in computing. Hence the scaling of $\tilde{\mathcal{D}}_2^x(r_1,r_2)$ is given by

$$\tilde{\mathcal{D}}_2^x(r_1,r_2) \sim \sum_N [1-e^{-2N\gamma}]P(r_1,r_2;N) \sim \begin{cases} r^{-1/4} & \text{(bulk)} \\ r^{-1/3} & \text{(boundary)}. \end{cases} \tag{41}$$

Thus, upon comparison with Eq. (21), we finally read off the multifractal exponent for $q=2$ as $\Delta_2^b=-1/4$ for the bulk and $\Delta_2^s=-1/3$ for the boundary. We will discuss the case of the wave-function scaling behavior at corners at the end (see Sec. VI) as it is a straightforward extension of the boundary case upon making use of conformal invariance. In Sec. IV C we consider the more interesting exponent describing the scaling of the third moment of the square of the wave functions' amplitude.

C. Calculation of Δ_3

The algebraic procedure for calculating the multifractal exponent Δ_q for $q=3$ is almost same as that we used above for $q=2$. Hence we present only the important steps and focus on the main results and the interesting differences. We start with the expression

$$\tilde{\mathcal{D}}_3^x(r_1,r_2,r_3) \propto \overline{\mathrm{tr}[G_R(r_1,r_1)-G_A(r_1,r_1)]\mathrm{tr}[G_R(r_2,r_2)-G_A(r_2,r_2)]\mathrm{tr}[G_R(r_3,r_3)-G_A(r_3,r_3)]}. \tag{42}$$

Converting all advanced Green's functions to retarded ones using Eq. (16), we can write the above equation as

$$\begin{aligned}\tilde{\mathcal{D}}_3^x(r_1,r_2,r_3) &\propto \overline{\mathrm{tr}[G(r_1,r_1)-1]\mathrm{tr}[G(r_2,r_2)-1]\mathrm{tr}[G(r_3,r_3)-1]} \\ &= \overline{\mathrm{tr}\, G(r_1,r_1)\mathrm{tr}\, G(r_2,r_2)\mathrm{tr}\, G(r_3,r_3)} - 1 \\ &\quad - \sum_{[r_1,r_2,r_3]} \overline{\mathrm{tr}\, G(r_1,r_1)\mathrm{tr}\, G(r_2,r_2)} \\ &\quad + \sum_{[r_1,r_2,r_3]} \overline{\mathrm{tr}\, G(r_1,r_1)}, \end{aligned} \tag{43}$$

where $\Sigma_{[r_1,r_2,r_3]}$ denotes sum over terms with all cyclic permutations of (r_1,r_2,r_3).

The new piece we have to evaluate here is the product of three Green's functions. For this consider the following two identities, obtained by applying Wick's theorem and valid in any fixed realization of disorder:

$$[G_{ij}G_{lm}+G_{im}G_{lj}]G_{kn} = \langle b_i b_j^\dagger b_l b_m^\dagger f_k f_n^\dagger\rangle. \tag{44}$$

Exchanging bosons and fermions in the above equation, we find

$$[G_{ij}G_{lm}-G_{im}G_{lj}]G_{kn} = \langle f_i f_j^\dagger f_l f_m^\dagger b_k b_n^\dagger\rangle. \tag{45}$$

In Eq. (44), let $i\to(r_1,\alpha_1)$, $j\to(r_1,\beta_1)$, $l\to(r_2,\alpha_2)$, $m\to(r_2,\beta_2)$, $k\to(r_3,\alpha_3)$, and $n\to(r_3,\beta_3)$, yielding

$$\begin{aligned}\mathrm{LHS} = [&G_{\beta_1}^{\alpha_1}(r_1,r_1)G_{\beta_2}^{\alpha_2}(r_2,r_2) \\ &+ G_{\beta_2}^{\alpha_1}(r_1,r_2)G_{\beta_1}^{\alpha_2}(r_2,r_1)]G_{\beta_3}^{\alpha_3}(r_3,r_3). \end{aligned} \tag{46}$$

As above, it is convenient to contract with the SU(2)-invariant $\delta_{\alpha_1}^{\beta_1}\delta_{\alpha_2}^{\beta_2}\delta_{\alpha_3}^{\beta_3}$, after performing the disorder average

$$\begin{aligned}&\overline{\mathrm{tr}\, G(r_1,r_1)\mathrm{tr}\, G(r_2,r_2)\mathrm{tr}\, G(r_3,r_3)} \\ &\quad + \overline{\mathrm{tr}\, G(r_3,r_3)\mathrm{tr}[G(r_1,r_2)G(r_2,r_1)]} \\ &\quad = \langle b_\alpha(r_1)b_\alpha^\dagger(r_1)b_\beta(r_2)b_\beta^\dagger(r_2)f_\gamma(r_3)f_\gamma^\dagger(r_3)\rangle \\ &\quad = \langle [1+2B(r_1)][1+2B(r_2)][1-2Q_3(r_3)]\rangle. \end{aligned} \tag{47}$$

We see that the first term on the LHS of Eq. (47) is the Green's-function product we want to evaluate in Eq. (43), while the second term has to be eliminated. This can be achieved by performing steps, analogous to those above, in Eq. (45), yielding

$$\begin{aligned}&\overline{\mathrm{tr}\, G(r_1,r_1)\mathrm{tr}\, G(r_2,r_2)\mathrm{tr}\, G(r_3,r_3)} \\ &\quad - \overline{\mathrm{tr}\, G(r_3,r_3)\mathrm{tr}[G(r_1,r_2)G(r_2,r_1)]} \\ &\quad = \langle f_\alpha(r_1)f_\alpha^\dagger(r_1)f_\beta(r_2)f_\beta^\dagger(r_2)b_\gamma(r_3)b_\gamma^\dagger(r_3)\rangle \\ &\quad = \langle [1-2Q_3(r_1)][1-2Q_3(r_2)][1+2B(r_3)]\rangle. \end{aligned} \tag{48}$$

Adding Eqs. (47) and (48), we obtain

$$\begin{aligned}&2\,\overline{\mathrm{tr}\, G(r_1,r_1)\mathrm{tr}\, G(r_2,r_2)\mathrm{tr}\, G(r_3,r_3)} \\ &\quad = \langle [1+2B(r_1)][1+2B(r_2)][1-2Q_3(r_3)] \\ &\quad + [1-2Q_3(r_1)][1-2Q_3(r_2)][1+2B(r_3)]\rangle. \end{aligned} \tag{49}$$

We can now use Eqs. (31), (33), and (49) to write Eq. (43) as

$$\begin{aligned}\tilde{\mathcal{D}}_3^x(r_1,r_2,r_3) \propto &\langle [1+2B(r_1)][1+2B(r_2)][1-2Q_3(r_3)] \\ &+ [1-2Q_3(r_1)][1-2Q_3(r_2)][1+2B(r_3)]\rangle \\ &- \sum_{[r_1,r_2,r_3]} \langle [1-2Q_3(r_1)][1+2B(r_2)]\rangle \\ &+ \sum_{[r_1,r_2,r_3]} \langle 1+2B(r_1)\rangle - 1. \end{aligned} \tag{50}$$

Converting these expressions to percolation probabilities is exactly analogous to the two-point case. Taking the critical limit $z\to 1$, we obtain

$$\tilde{\mathcal{D}}_3^x(r_1,r_2,r_3) \propto P(r_1,r_2,r_3) + P(r_1,r_3,r_2), \tag{51}$$

where $P(r_1,r_2,r_3)$ is the probability of a loop of any size traversing r_1, r_2, and r_3 in that order. There is no cancellation to leading order at criticality here, unlike the two-point case. The final scaling of this correlator is simply given by that of the usual three-point correlation function of percolation one-hull operators at criticality,

$$P(r_1,r_2,r_3), P(r_1,r_3,r_2) \sim \begin{cases} r^{-3x_b} \sim r^{-3/4} & \text{(bulk)} \\ r^{-3x_s} \sim r^{-1} & \text{(boundary)}. \end{cases} \tag{52}$$

Hence the value of multifractal exponent for $q=3$ is $\Delta_3^b = -3/4$ and $\Delta_3^s = -1$, for bulk and boundary, respectively.

D. Higher multifractal exponents

The procedure for calculating Δ_3^x was very similar to that of Δ_2^x (albeit more tedious) and one might ask if it can be extended to higher multifractal exponents, Δ_q^x with $q>3$. On the other hand however, the fact that we are able to calculate Δ_3^x at all using our formalism is conceptually surprising because usually in supersymmetric problems, an additional set (="replica") of boson and fermion operators is required for each additional Green's-function factor entering the product in Eq. (24). Here we are able to calculate both two- and three-point functions with the same number of boson and fermion operators (replicas).

To understand this, we look at the calculation of Δ_3 carefully. We had an extra "unwanted" Green's-function product in Eq. (47). But we were able to eliminate it by using an equation similar to Eq. (48), with bosons and fermions exchanged. The unwanted Green's-function product canceled between Eq. (47) and Eq. (48) when added together, giving us the exact product that we wanted.

Now does such a cancellation go through for higher-point functions? To answer this, we look at the next higher exponent, Δ_4^x. Here we will have to evaluate a product of four Green's functions,

$$\overline{\mathrm{tr}\, G(r_1,r_1)\mathrm{tr}\, G(r_2,r_2)\mathrm{tr}\, G(r_3,r_3)\mathrm{tr}\, G(r_4,r_4)}.$$

To evaluate this, we will have to use the following identity obtained from Wick's theorem (in a fixed realization of disorder):

$$[G_{ij}G_{lm} - G_{im}G_{lj}][G_{pq}G_{rs} + G_{ps}G_{rq}] = \langle f_i f_j^\dagger f_l f_m^\dagger b_p b_q^\dagger b_r b_s^\dagger \rangle. \tag{53}$$

In this equation, let again $i \to (r_1,\alpha_1)$, $j \to (r_1,\beta_1)$, $l \to (r_2,\alpha_2)$, $m \to (r_2,\beta_2)$, $p \to (r_3,\alpha_3)$, $q \to (r_3,\beta_3)$, $r \to (r_4,\alpha_4)$, and $s \to (r_4,\beta_4)$. Then contracting with the SU(2)-invariant $\delta_{\alpha_1}^{\beta_1}\delta_{\alpha_2}^{\beta_2}\delta_{\alpha_3}^{\beta_3}\delta_{\alpha_4}^{\beta_4}$ gives us upon averaging the relation

$$\begin{aligned}
&\overline{\mathrm{tr}\, G(r_1,r_1)\mathrm{tr}\, G(r_2,r_2)\mathrm{tr}\, G(r_3,r_3)\mathrm{tr}\, G(r_4,r_4)} \\
&\quad + \overline{\mathrm{tr}\, G(r_1,r_1)\mathrm{tr}\, G(r_2,r_2)\mathrm{tr}[G(r_3,r_4)G(r_4,r_3)]} \\
&\quad - \overline{\mathrm{tr}[G(r_1,r_2)G(r_2,r_1)]\mathrm{tr}\, G(r_3,r_3)\mathrm{tr}\, G(r_4,r_4)} \\
&\quad - \overline{\mathrm{tr}[G(r_1,r_2)G(r_2,r_1)]\mathrm{tr}[G(r_3,r_4)G(r_4,r_3)]} \\
&\quad = \langle [1-2Q_3(r_1)][1-2Q_3(r_2)][1+2B(r_3)][1+2B(r_4)]\rangle.
\end{aligned} \tag{54}$$

There are three unwanted terms on the LHS. Exchanging bosons and fermions gives on the other hand

$$\begin{aligned}
&\overline{\mathrm{tr}\, G(r_1,r_1)\mathrm{tr}\, G(r_2,r_2)\mathrm{tr}\, G(r_3,r_3)\mathrm{tr}\, G(r_4,r_4)} \\
&\quad - \overline{\mathrm{tr}\, G(r_1,r_1)\mathrm{tr}\, G(r_2,r_2)\mathrm{tr}[G(r_3,r_4)G(r_4,r_3)]} \\
&\quad + \overline{\mathrm{tr}[G(r_1,r_2)G(r_2,r_1)]\mathrm{tr}\, G(r_3,r_3)\mathrm{tr}\, G(r_4,r_4)} \\
&\quad - \overline{\mathrm{tr}[G(r_1,r_2)G(r_2,r_1)]\mathrm{tr}[G(r_3,r_4)G(r_4,r_3)]} \\
&\quad = \langle [1-2Q_3(r_3)][1-2Q_3(r_4)][1+2B(r_1)][1+2B(r_2)]\rangle.
\end{aligned} \tag{55}$$

Adding Eqs. (54) and (55) eliminates two unwanted pieces:

$$\begin{aligned}
&2\,\overline{\mathrm{tr}\, G(r_1,r_1)\mathrm{tr}\, G(r_2,r_2)\mathrm{tr}\, G(r_3,r_3)\mathrm{tr}\, G(r_4,r_4)} \\
&\quad - 2\,\overline{\mathrm{tr}[G(r_1,r_2)G(r_2,r_1)]\mathrm{tr}[G(r_3,r_4)G(r_4,r_3)]} \\
&\quad = \langle [1+2B(r_1)][1+2B(r_2)][1-2Q_3(r_3)][1-2Q_3(r_4)]\rangle \\
&\quad + \langle [1-2Q_3(r_1)][1-2Q_3(r_2)][1+2B(r_3)][1+2B(r_4)]\rangle.
\end{aligned} \tag{56}$$

We are still left with one unwanted piece which cannot be evaluated or canceled with something else. Any other combination of the generators of the Lie superalgebra at four points will generate more terms on applying Wick's theorem and cannot be canceled out.

Now we see the special feature of the three-point calculation. We had two Green's-function products (by applying Wick's theorem), of which only one was necessary. The supersymmetric formulation gave us one more equation due to boson-fermion interchangeability. The unwanted piece canceled between the fermionic and bosonic equations. This fact does not help us in higher-correlation functions as they have more unwanted pieces. It is also clear that situation becomes worse for higher n-point functions. Interestingly, the same conclusion was reached in a very different way in Ref. 30.

V. LOCAL DENSITY OF STATES AND POINT-CONTACT CONDUCTANCE

Having considered the multifractal calculation in detail, the calculation of other boundary critical exponents is completely analogous and we list only the important results. Some of the bulk exponents were found in Refs. 17, 30, and 46 using a very different technique. The averaged local density of states (LDOS), summed over the spin indices, can be written in terms of Green's functions as

$$\langle \rho^x(r,\epsilon)\rangle = \frac{1}{4\pi}\overline{\mathrm{tr}[G_R(r,r) - G_A(r,r)]} = \frac{1}{2\pi}\overline{\mathrm{tr}\, G_R(r,r) - 1}. \tag{57}$$

This can again be expressed in terms of the sl(2|1) supersymmetry generators as $(1/2\pi)\langle 2B(r)\rangle$. This average, following the same steps presented in Sec. IV B, can be written in terms of percolation probabilities as

$$\langle 2B(r)\rangle = 1 - \sum_N P(r;N)\cos 2N\epsilon. \tag{58}$$

(The same result was also obtained in Ref. 46 using, as mentioned, different techniques.) As we have mentioned at the end of Sec. III, the boundary and the bulk scaling dimensions of the one-hull operator are $x_s = 1/3$ and $x_b = 1/4$. The latter value implies that the percolation hull has fractal dimension $2-x_b = 7/4$, so that $P(r,N) \sim N^{-8/7}$ for r in bulk. This yields, according to Eq. (57), the following scaling behavior of the LDOS:[17]

$$\rho^b(\epsilon) \propto \epsilon^{x_b/(2-x_b)} = \epsilon^{1/7}. \tag{59}$$

Note that $2-x_b = 7/4$ is the dynamic critical exponent governing the scaling of energy with the system size L at SQH criticality, so that the level spacing at $\epsilon = 0$ (and thus the characteristic energy of critical states) is $\delta \sim L^{-7/4}$. In our case, when the point r is located at the boundary, we find

$$P(r,N) \sim N^{-1-x_s/(2-x_b)} = N^{-25/21}, \tag{60}$$

and the LDOS scaling

$$\rho^s(r,\epsilon) \propto \epsilon^{x_s/(2-x_b)} = \epsilon^{4/21}. \tag{61}$$

Here we have used the bulk dynamic critical exponent in determining the energy scaling of the boundary LDOS. This is because we are dealing with an "ordinary surface transition" and here surface (boundary) criticality is driven by the divergence of the bulk correlation length.[31] Thus the scaling of LDOS changes between bulk and boundary. This means, as was mentioned in Sec. IV A, that the average of the (square of the) wave-function amplitude is suppressed at the boundary, giving rise to a nonvanishing value of $\mu_{x=s} = 1/3 - 1/4 = 1/12$ [see Eq. (19)].

A similar procedure is adopted for the calculation of other boundary exponents (we give a table of all exponents later).

The boundary diffusion propagator can be written as

$$\langle \Pi_{ss}(r_1,r_2)\rangle = 2\langle V_-(r_1)W_+(r_2)\rangle, \tag{62}$$

where r_1 and r_2 lie at the boundary. In terms of percolation probabilities this reads

$$\langle \Pi_{ss}(r_1,r_2)\rangle = 2\sum_N P(r_1,r_2;N)z^{2N}. \tag{63}$$

Taking the limit $z\to 1$ (critical point) gives

$$\langle \Pi_{ss}(r_1,r_2)\rangle = 2\sum_N P(r_1,r_2;N) = 2P(r_1,r_2). \tag{64}$$

Here the probability $P(r_1,r_2)$ for the points r_1 and r_2 to be connected by a hull of any length scales at the boundary as r^{-2x_s}, giving

$$\langle \Pi_{ss}(r_1,r_2)\rangle \sim |r_1-r_2|^{-2/3}. \tag{65}$$

Another physical quantity of interest is the boundary point-contact conductance. In a network model setting, this is defined as the conductance between two boundary links r_1 and r_2 which are cut to make it possible to insert and extract currents from them.[52] In the second-quantized formalism, this is equivalent to creating a boson (or alternately a fermion because of the supersymmetry) for each spin direction at one link and destroying the same particle at another link. This translates to the expression

$$\langle g_{\text{point}}(r_1,r_2)\rangle \equiv \langle f_\uparrow^\dagger(r_1)f_\downarrow^\dagger(r_1)f_\downarrow(r_2)f_\uparrow(r_2)\rangle. \tag{66}$$

In terms of sl(2|1) generators, this equals $\langle Q_+(r_1)Q_-(r_2)\rangle$. Skipping here the mapping to percolation probabilities, we find that the point-contact conductance decays exactly in the same way as the diffusion propagator and, in particular, scales as $|r_1-r_2|^{-2/3}$ at the boundary, at criticality. This result is expected since the correlators for the diffusion propagator and the point-contact conductance represent different superspin components in the same representation of the superalgebra sl(2|1).

VI. EXPONENTS IN OTHER GEOMETRIES

There are two distinct ways of extending our discussion of boundary behavior. The first one is when some of the points lie on the boundary while the others lie in the bulk. The other case is to consider boundaries with more complicated geometries, the simplest example of which would be a wedge with opening angle θ. (The boundary case, considered in Secs. III–V, corresponds to $\theta=\pi$.)

The two-point quantities are easily computed when one point r_1 lies in the bulk and the other point, r_2 is at the boundary. These scale as $r^{-(\eta_b+\eta_\parallel)/2}$, where η_b and $\eta_\parallel$ are the usual exponents giving the decay of the two-point function in the bulk and along the boundary, respectively. Hence the diffusion propagator and the point-contact conductance between a point in the bulk and another at the boundary, both scale with distance r as $r^{-7/12}$.

In the case of multifractal exponents, we can calculate the scaling behavior of correlation functions similar to those in Eq. (24). But we should not interpret these as representing properties of a single multifractal since multifractality is essentially a single-point property. With this caveat, the value of the quantity analogous to Δ_2 when one point is in the bulk and another is at the boundary is $-1/4$.

TABLE I. One-point exponents in various geometries: bulk, near straight boundaries, and near corners. The first line indicates the scaling behavior of the LDOS at the SQH transition. The second and third lines represent the multifractal-scaling exponents for the second and third moments of the critical wave-function intensity.

Geometry	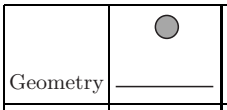		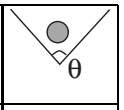
LDOS	$\epsilon^{1/7}$	$\epsilon^{4/21}$	$\epsilon^{(4/21)(\pi/\theta)}$
Δ_2	$-1/4$	$-1/3$	$-\pi/3\theta$
Δ_3	$-3/4$	-1	$-\pi/\theta$

The next generalization is to analyze the SQH transition in a wedge geometry. This can be readily carried out using conformal invariance arguments.[35] The conformal transformation $w=z^{\theta/\pi}$ maps the boundary geometry on the z plane to a wedge of opening angle θ on the w plane. From this, it can be deduced that if we consider a two-point function with one point lying near the wedge tip and another deep in the bulk at distance r, the two-point function decays as $r^{-\eta_\theta}$, where

$$\eta_\theta = x_b + \frac{\pi}{\theta}x_s. \tag{67}$$

This enables us to calculate the relevant exponents. In the density-of-states calculation, we will have to replace x_s with $(\pi/\theta)x_s$.

VII. CONCLUSIONS AND OUTLOOK

The central result of this paper is the calculation of boundary critical and multifractal exponents for the spin quantum Hall transition in various geometries. (See Tables I and II for a summary of results.) In this paper, we have confined ourselves to the exact calculation of anomalous multifractal dimensions for low-moment order q, using the percolation mapping. In general, in the theory of multifractality, the information contained in the set of all the critical exponents τ_q^x defined in Eq. (18) can also be expressed in terms of the so-called singularity spectrum $f_x(\alpha)$, its Leg-

TABLE II. Critical scaling behavior of the diffusion propagator $\Pi(r_1,r_2)$ in various geometries. The point-contact conductance has an identical scaling behavior as indicated in the text.

Geometry	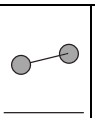	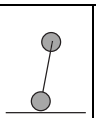	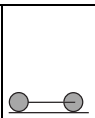	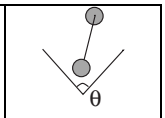
$\Pi(r_1,r_2)$	$r^{-1/2}$	$r^{-7/12}$	$r^{-2/3}$	$r^{-1/4-(1/3)(\pi/\theta)}$

endre transform. We remark that in the presence of a boundary, the singularity spectrum concept has to be understood more broadly. This is because unlike in ordinary critical phenomena, the presence of a boundary can affect the singularity spectrum (and τ_q^x) of the entire system, including bulk and boundaries, in a significant way, even in the thermodynamic limit. These issues were first pointed out in Ref. 36 and were analyzed therein, as well as in Refs. 26 and 53.

The analysis of multifractality in various other geometries leads to interesting new concepts. Some of these ideas have been explored for the Anderson transition in $d=2+\epsilon$,[36] power-law random banded matrices,[54] and the 2D symplectic class transition,[26,53] all of which display the characteristic multifractal property of LD critical points. A similar study of Dirac fermions in random gauge fields[55] and the integer quantum Hall transitions in two dimensions is expected to further our understanding of boundary multifractality and provide important clues regarding the structure of some of the unknown bulk theories.

ACKNOWLEDGMENTS

We thank N. Read for initial discussions of boundary MF at the SQH transition and A. D. Mirlin for a previous collaboration on boundary MF. This work was supported in part by the Chandrasekhar and Sachs Grants (A.R.S.), NSF Grant No. DMR-0448820, NSF MRSEC Grant No. DMR-0213745, the Alfred P. Sloan Foundation and the Research Corporation (I.A.G.), and NSF Grant No. DMR-0706140 (A.W.W.L.).

APPENDIX A: REPRESENTATIONS OF sl(2|1) SUPERALGEBRA

The sl(2|1) superalgebra has eight generators, of which four are bosonic (B,Q_3,Q_+,Q_-) and four are fermionic (V_+,V_-,W_+,W_-). We use the convention of Ref. 56 for the generators. These satisfy the same commutation ([,]) and anticommutation ({,}) relations as the generators of osp(2|2) superalgebra:

$$[B,Q_3]=[B,Q_\pm]=0,$$

$$[B,V_\pm]=\frac{1}{2}V_\pm,\quad [B,W_\pm]=-\frac{1}{2}W_\pm,$$

$$[Q_3,Q_\pm]=\pm Q_\pm,\quad [Q_+,Q_-]=2Q_3,$$

$$[Q_3,V_\pm]=\pm\frac{1}{2}V_\pm,\quad [Q_3,W_\pm]=\pm\frac{1}{2}W_\pm,$$

$$[Q_+,V_-]=V_+,\quad [Q_+,W_-]=W_+,$$

$$[Q_-,V_+]=V_-,\quad [Q_-,W_+]=W_-,$$

$$[Q_+,V_+]=[Q_+,W_+]=[Q_-,V_-]=[Q_-,W_-]=0,$$

$$\{V_+,V_-\}=\{W_+,W_-\}=0,$$

$$\{V_+,W_+\}=Q_+,\quad \{V_+,W_-\}=B-Q_3,$$

$$\{V_-,W_-\}=-Q_-,\quad \{V_-,W_+\}=-B-Q_3. \tag{A1}$$

An important subalgebra is gl(1|1) formed by the generators (B,Q_3,V_-,W_+). This is the SUSY present in the SQH network at finite broadening γ, when $z=e^{-\gamma}<1$ (see Eqs. (14) and (15)], as well as at an absorbing boundary.

The sl(2|1) algebra has an oscillator realization formed by bilinear combinations of the fermion and boson operators on each link that are SU(2) singlets. For the up links the oscillator representation is

$$Q_3=\frac{1}{2}(f_\uparrow^\dagger f_\uparrow+f_\downarrow^\dagger f_\downarrow-1),$$

$$Q_+=f_\uparrow^\dagger f_\downarrow^\dagger,\quad Q_-=f_\downarrow f_\uparrow,$$

$$B=\frac{1}{2}(b_\uparrow^\dagger b_\uparrow+b_\downarrow^\dagger b_\downarrow+1),$$

$$V_+=\frac{1}{\sqrt{2}}(b_\uparrow^\dagger f_\downarrow^\dagger-b_\downarrow^\dagger f_\uparrow^\dagger),$$

$$V_-=-\frac{1}{\sqrt{2}}(b_\uparrow^\dagger f_\uparrow+b_\downarrow^\dagger f_\downarrow),$$

$$W_+=\frac{1}{\sqrt{2}}(f_\uparrow^\dagger b_\uparrow+f_\downarrow^\dagger b_\downarrow),$$

$$W_-=\frac{1}{\sqrt{2}}(b_\uparrow f_\downarrow-b_\downarrow f_\uparrow). \tag{A2}$$

These operators act irreducibly in the fundamental three-dimensional representation of sl(2|1) (denoted by **3**) with the space of states spanned by three SU(2) singlet states which we denote as $|m\rangle$, $m=0,1,2$:

$$|0\rangle=|\text{vacuum}\rangle, \tag{A3}$$

$$|1\rangle=V_+|0\rangle=\frac{1}{\sqrt{2}}(b_\uparrow^\dagger f_\downarrow^\dagger-b_\downarrow^\dagger f_\uparrow^\dagger)|0\rangle, \tag{A4}$$

$$|2\rangle=Q_+|0\rangle=f_\uparrow^\dagger f_\downarrow^\dagger|0\rangle. \tag{A5}$$

We need the matrix elements of the sl(2|1) generators between the states in **3**. The nonzero matrix elements are easy to find from the following equations giving the action of the generators on the states:

$$Q_3|0\rangle=-\frac{1}{2}|0\rangle,\quad Q_3|1\rangle=0,\quad Q_3|2\rangle=\frac{1}{2}|2\rangle,$$

$$B|0\rangle=\frac{1}{2}|0\rangle,\quad B|1\rangle=|1\rangle,\quad B|2\rangle=\frac{1}{2}|2\rangle,$$

$$Q_+|0\rangle=|2\rangle,\quad Q_-|2\rangle=|0\rangle,$$

$$V_+|0\rangle = |1\rangle, \quad V_-|2\rangle = -|1\rangle,$$

$$W_+|1\rangle = |2\rangle, \quad W_-|1\rangle = |0\rangle. \tag{A6}$$

These equations give us the matrices of the generators of sl(2|1) in the fundamental representation (for a generator G the matrix elements G_{ij}, $i,j=1,2,3$, are defined by $G|i\rangle = \Sigma_j G_{ji}|j\rangle$):

$$B = \begin{pmatrix} 1/2 & 0 & 0 \\ 0 & 1 & 0 \\ 0 & 0 & 1/2 \end{pmatrix}, \quad Q_3 = \begin{pmatrix} -1/2 & 0 & 0 \\ 0 & 0 & 0 \\ 0 & 0 & 1/2 \end{pmatrix},$$

$$Q_+ = \begin{pmatrix} 0 & 0 & 0 \\ 0 & 0 & 0 \\ 1 & 0 & 0 \end{pmatrix}, \quad Q_- = \begin{pmatrix} 0 & 0 & 1 \\ 0 & 0 & 0 \\ 0 & 0 & 0 \end{pmatrix},$$

$$V_+ = \begin{pmatrix} 0 & 0 & 0 \\ 1 & 0 & 0 \\ 0 & 0 & 0 \end{pmatrix}, \quad W_- = \begin{pmatrix} 0 & 1 & 0 \\ 0 & 0 & 0 \\ 0 & 0 & 0 \end{pmatrix},$$

$$V_- = \begin{pmatrix} 0 & 0 & 0 \\ 0 & 0 & -1 \\ 0 & 0 & 0 \end{pmatrix}, \quad W_+ = \begin{pmatrix} 0 & 0 & 0 \\ 0 & 0 & 0 \\ 0 & 1 & 0 \end{pmatrix}. \tag{A7}$$

In Fig. 2 we give the weight diagrams for the fundamental and adjoint representations which are useful for understanding some of our arguments.

For the down links the construction is similar. The oscillator realization of the sl(2|1) generators is now

$$\bar{Q}_3 = \frac{1}{2}(\bar{f}_\uparrow^\dagger \bar{f}_\uparrow + \bar{f}_\downarrow^\dagger \bar{f}_\downarrow + 1),$$

$$\bar{Q}_+ = \bar{f}_\downarrow \bar{f}_\uparrow, \quad \bar{Q}_- = \bar{f}_\uparrow^\dagger \bar{f}_\downarrow^\dagger,$$

$$\bar{B} = -\frac{1}{2}(\bar{b}_\uparrow^\dagger \bar{b}_\uparrow + \bar{b}_\downarrow^\dagger \bar{b}_\downarrow + 1),$$

$$\bar{V}_+ = \frac{1}{\sqrt{2}}(\bar{b}_\downarrow \bar{f}_\uparrow - \bar{b}_\uparrow \bar{f}_\downarrow),$$

$$\bar{V}_- = \frac{1}{\sqrt{2}}(\bar{f}_\uparrow^\dagger \bar{b}_\uparrow + \bar{f}_\downarrow^\dagger \bar{b}_\downarrow),$$

$$\bar{W}_+ = -\frac{1}{\sqrt{2}}(\bar{b}_\uparrow^\dagger \bar{f}_\uparrow + \bar{b}_\downarrow^\dagger \bar{f}_\downarrow),$$

$$\bar{W}_- = \frac{1}{\sqrt{2}}(\bar{b}_\downarrow^\dagger \bar{f}_\uparrow^\dagger - \bar{b}_\uparrow^\dagger \bar{f}_\downarrow^\dagger). \tag{A8}$$

These operators satisfy the same commutation relations as the ones on the up links and act in the three-dimensional space spanned by the SU(2) singlets

$$|\bar{0}\rangle = |\text{vacuum}\rangle,$$

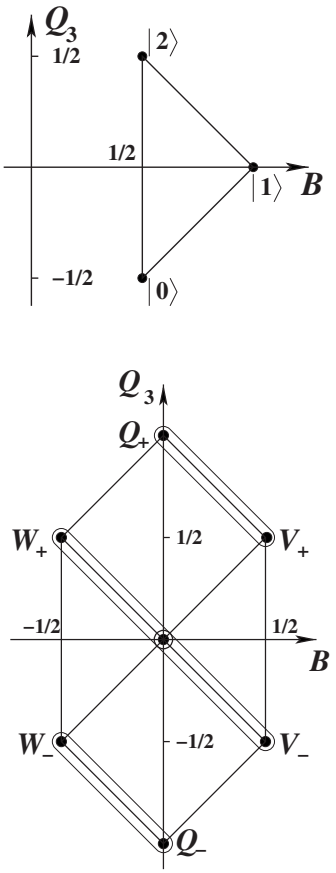

FIG. 2. Weight diagrams of sl(2|1). We show two doublets and the adjoint of the subalgebra gl(1|1) in the adjoint representation diagram.

$$|\bar{1}\rangle = -\bar{W}_-|\bar{0}\rangle = \frac{1}{\sqrt{2}}(\bar{b}_\uparrow^\dagger \bar{f}_\downarrow^\dagger - \bar{b}_\downarrow^\dagger \bar{f}_\uparrow^\dagger)|\bar{0}\rangle,$$

$$|\bar{2}\rangle = -\bar{Q}_-|\bar{0}\rangle = -\bar{f}_\uparrow^\dagger \bar{f}_\downarrow^\dagger |\bar{0}\rangle. \tag{A9}$$

These singlets form the representation $\bar{\mathbf{3}}$ of the sl(2|1) algebra dual to the fundamental **3**. Note that the state $|\bar{1}\rangle$ contains odd number of fermions and, therefore, has negative square norm:

$$\langle \bar{1}|\bar{1}\rangle = -1. \tag{A10}$$

The action of the generators on the states in the representation $\bar{\mathbf{3}}$ is easily found to be

$$\bar{Q}_3|\bar{0}\rangle = \frac{1}{2}|\bar{0}\rangle, \quad \bar{Q}_3|\bar{1}\rangle = 0, \quad \bar{Q}_3|\bar{2}\rangle = -\frac{1}{2}|\bar{2}\rangle,$$

$$\bar{B}|\bar{0}\rangle = -\frac{1}{2}|\bar{0}\rangle, \quad \bar{B}|\bar{1}\rangle = -|\bar{1}\rangle, \quad \bar{B}|\bar{2}\rangle = -\frac{1}{2}|\bar{2}\rangle,$$

$$\bar{Q}_+|\bar{2}\rangle = -|\bar{0}\rangle, \quad \bar{Q}_-|\bar{0}\rangle = -|\bar{2}\rangle,$$

$$\bar{V}_+|\bar{1}\rangle = |\bar{0}\rangle, \quad \bar{V}_-|\bar{1}\rangle = -|\bar{2}\rangle,$$

$$\bar{W}_+|\bar{2}\rangle = -|\bar{1}\rangle, \quad \bar{W}_-|\bar{0}\rangle = -|\bar{1}\rangle. \tag{A11}$$

This gives the matrices for the generators in $\bar{\mathbf{3}}$:

$$\bar{B} = \begin{pmatrix} -1/2 & 0 & 0 \\ 0 & -1 & 0 \\ 0 & 0 & -1/2 \end{pmatrix}, \quad \bar{Q}_3 = \begin{pmatrix} 1/2 & 0 & 0 \\ 0 & 0 & 0 \\ 0 & 0 & -1/2 \end{pmatrix},$$

$$\bar{Q}_+ = \begin{pmatrix} 0 & 0 & -1 \\ 0 & 0 & 0 \\ 0 & 0 & 0 \end{pmatrix}, \quad \bar{Q}_- = \begin{pmatrix} 0 & 0 & 0 \\ 0 & 0 & 0 \\ -1 & 0 & 0 \end{pmatrix},$$

$$\bar{V}_+ = \begin{pmatrix} 0 & 1 & 0 \\ 0 & 0 & 0 \\ 0 & 0 & 0 \end{pmatrix}, \quad \bar{W}_- = \begin{pmatrix} 0 & 0 & 0 \\ -1 & 0 & 0 \\ 0 & 0 & 0 \end{pmatrix},$$

$$\bar{V}_- = \begin{pmatrix} 0 & 0 & 0 \\ 0 & 0 & 0 \\ 0 & -1 & 0 \end{pmatrix}, \quad \bar{W}_+ = \begin{pmatrix} 0 & 0 & 0 \\ 0 & 0 & -1 \\ 0 & 0 & 0 \end{pmatrix}. \tag{A12}$$

APPENDIX B: BOUNDARY SUSY

We demonstrate in this appendix that the introduction of a reflecting boundary preserves the full sl(2|1) SUSY. First we note some useful relations satisfied by the bosons and fermions defined in Sec. III C. For any function F, all bosons and fermions (denoted by $c, c^\dagger$) except the negative norm ones satisfy the commutation relations

$$[c, :F(c^\dagger, c):] = :\frac{\vec{\partial}}{\partial c^\dagger} F(c^\dagger, c):,$$

$$[c^\dagger, :F(c^\dagger, c):] = -:F(c^\dagger, c)\frac{\overleftarrow{\partial}}{\partial c}:, \tag{B1}$$

where the :: denotes normal ordering. The negative norm operators satisfy

$$[c, :F(c^\dagger, c):] = -:\frac{\vec{\partial}}{\partial c^\dagger} F(c^\dagger, c):,$$

$$[c^\dagger, :F(c^\dagger, c):] = :F(c^\dagger, c)\frac{\overleftarrow{\partial}}{\partial c}:. \tag{B2}$$

One can first write the transfer matrix for a single A node in the bulk.[57] Since the scattering at the node is diagonal in spin indices [see Eq. (12)], the node transfer matrices are products of two independent transfer matrices for each spin direction:

$$T_A = \prod_{\sigma=\uparrow,\downarrow} T_{A\sigma} = T_{A\uparrow} T_{A\downarrow}, \tag{B3}$$

where

$$T_{A\sigma} = \exp[t_{A\sigma}(f_\sigma^\dagger \bar{f}_\sigma^\dagger + b_\sigma^\dagger \bar{b}_\sigma^\dagger)](1 - t_{A\sigma}^2)^{(1/2)n_\sigma} \times \exp[-t_{A\sigma}(\bar{f}_\sigma f_\sigma + \bar{b}_\sigma b_\sigma)], \tag{B4}$$

$$n_\sigma = n_{f\sigma} + n_{b\sigma} + n_{\bar{f}\sigma} + n_{\bar{b}\sigma}. \tag{B5}$$

Let us also introduce the notation

$$T_+ = \prod_\sigma \exp[t_{A\sigma}(f_\sigma^\dagger \bar{f}_\sigma^\dagger + b_\sigma^\dagger \bar{b}_\sigma^\dagger)], \tag{B6}$$

$$T_0 = \prod_\sigma (1 - t_{A\sigma}^2)^{(1/2)n_\sigma}, \tag{B7}$$

$$T_- = \prod_\sigma \exp[-t_{A\sigma}(\bar{f}_\sigma f_\sigma + \bar{b}_\sigma b_\sigma)], \tag{B8}$$

so that $T_A = T_+ T_0 T_-$.

The three terms correspond respectively to the creation, propagation, and destruction of boson and fermions on evolution along the vertical direction. Similar expressions can also be written for the B nodes. In the spin-rotation-invariant case for any *particular* realization of the disorder in the scattering matrices, using the relations in Eqs. (B1) and (B2), it can be checked that each node transfer matrix in Eq. (B3) commutes with the sum of the eight generators of the superalgebra sl(2|1) ≅ osp(2|2) (see Appendix A) defined on the up link and down link on which the node transfer matrix acts.

Having defined the bulk nodes, we now consider the network on a semi-infinite half plane with a fully reflecting boundary either along the horizontal direction or the vertical direction. Although it is clear that physical quantities cannot depend on whether the boundary is defined along the horizontal or the vertical direction, the two cases have to be studied very differently within the second-quantized formalism. This is because of the fact that we have singled out the vertical direction as time and the tensor product of Fock spaces on which U_A and U_B act is defined along a particular horizontal row of links. For definiteness, let us assume that the boundary is always composed of A nodes.

We first consider the case of a reflecting boundary along the vertical (time) direction as shown in Fig. 1. In this case, we retain the periodic boundary condition along the time direction and hence also the supertrace STr in the correlation functions. Only the node transfer matrices on the boundary have to be changed to account for the complete reflection at the boundary. This can be implemented by setting $t_A = 0$ in Eq. (B4). In this case, the boundary node transfer matrix reduces to the trivial identity operator. Consequently the operators U_A and U_B still commute with all generators of the sl(2|1) superalgebra.

As mentioned before, we could have equivalently chosen the boundary to be along the horizontal-space direction, that is, along a single time slice. In this case, we will have to first replace the supertrace STr with the matrix element with respect to the global vacuum state $|0\rangle$. Next we will have to modify all the node transfer matrices along the boundary by setting $t_A = 1$ in Eq. (B4) and also consider only T_+ since no bosons or fermions can be created or propagated across the boundary. Note that the 90° rotation of the boundary changes the corresponding t_A. Hence the single-spin single node transfer matrix at the boundary is

$$T_A = \prod_{\sigma} \exp[(f_{\sigma}^{\dagger}\bar{f}_{\sigma}^{\dagger} + b_{\sigma}^{\dagger}\bar{b}_{\sigma}^{\dagger})]. \quad \text{(B9)}$$

This operator commutes only with the four elements $B+\bar{B}$, $Q_3+\bar{Q}_3$, $W_+ + \bar{W}_+$, and $V_- + \bar{V}_-$ which form the subalgebra gl(1|1). This seems to contradict the previous observation that a reflecting boundary along the vertical direction preserves the full sl(2|1) SUSY. This is reconciled by the fact that in the former case, we took the supertrace STr with a trivial boundary node transfer matrix, while here we need to consider the action of the boundary transfer matrix T_A in Eq. (B9) on the global vacuum $|0\rangle$. Using the relations in Eqs. (B1) and (B2), we can check that the state $T_A|0\rangle$ is a singlet under the action of the sl(2|1) symmetry on the two links involved. That is, it is annihilated by the sum over two links of all eight generators of the sl(2|1) superalgebra. Thus the full supersymmetry is restored within a lattice spacing from the boundary and the result matches with the previous case. For simplicity, in the main text, we always assume that the boundary is along the vertical direction as shown in Fig. 1. This enables us to retain the global supertrace STr in all the expressions.

[1] P. W. Anderson, Phys. Rev. **109**, 1492 (1958).
[2] E. Abrahams, P. W. Anderson, D. C. Licciardello, and T. V. Ramakrishnan, Phys. Rev. Lett. **42**, 673 (1979).
[3] F. Wegner, Z. Phys. B **35**, 207 (1979).
[4] K. B. Efetov, Adv. Phys. **32**, 53 (1983).
[5] K. Efetov, *Supersymmetry in Disorder and Chaos* (Cambridge University Press, Cambridge, 1997).
[6] A. D. Mirlin, Phys. Rep. **326**, 259 (2000); arXiv:cond-mat/9907126; F. Evers and A. D. Mirlin, Rev. Mod. Phys. **80**, 1355 (2008); arXiv:0707.4378.
[7] H. Levine, S. B. Libby, and A. M. M. Pruisken, Phys. Rev. Lett. **51**, 1915 (1983).
[8] S. Hikami, A. I. Larkin, and Y. Nagaoka, Prog. Theor. Phys. **63**, 707 (1980).
[9] M. R. Zirnbauer, J. Math. Phys. **37**, 4986 (1996); arXiv:math-ph/9808012.
[10] A. Altland and M. R. Zirnbauer, Phys. Rev. B **55**, 1142 (1997); arXiv:cond-mat/9602137.
[11] A. W. W. Ludwig, M. P. A. Fisher, R. Shankar, and G. Grinstein, Phys. Rev. B **50**, 7526 (1994).
[12] A. A. Nersesyan, A. M. Tsvelik, and F. Wenger, Phys. Rev. Lett. **72**, 2628 (1994); arXiv:cond-mat/9401026.
[13] C. Mudry, C. Chamon, and X.-G. Wen, Nucl. Phys. B **466**, 383 (1996); arXiv:cond-mat/9509054.
[14] T. Senthil, M. P. A. Fisher, L. Balents, and C. Nayak, Phys. Rev. Lett. **81**, 4704 (1998); arXiv:cond-mat/9808001.
[15] V. Kagalovsky, B. Horovitz, Y. Avishai, and J. T. Chalker, Phys. Rev. Lett. **82**, 3516 (1999); arXiv:cond-mat/9812155.
[16] T. Senthil, J. B. Marston, and M. P. A. Fisher, Phys. Rev. B **60**, 4245 (1999); arXiv:cond-mat/9902062.
[17] I. A. Gruzberg, A. W. W. Ludwig, and N. Read, Phys. Rev. Lett. **82**, 4524 (1999); arXiv:cond-mat/9902063.
[18] S. Guruswamy, A. LeClair, and A. W. W. Ludwig, Nucl. Phys. B **583**, 475 (2000); arXiv:cond-mat/9909143.
[19] C. Castellani and L. Peliti, J. Phys. A **19**, L429 (1986).
[20] M. Janssen, Int. J. Mod. Phys. B **8**, 943 (1994).
[21] B. Huckestein, Rev. Mod. Phys. **67**, 357 (1995).
[22] B. Duplantier and A. W. W. Ludwig, Phys. Rev. Lett. **66**, 247 (1991).
[23] A. A. Belavin, A. M. Polyakov, and A. B. Zamolodchikov, Nucl. Phys. B **241**, 333 (1984).
[24] F. Evers, A. Mildenberger, and A. D. Mirlin, Phys. Rev. B **64**, 241303(R) (2001).
[25] A. Mildenberger and F. Evers, Phys. Rev. B **75**, 041303(R) (2007).
[26] H. Obuse, A. R. Subramaniam, A. Furusaki, I. A. Gruzberg, and A. W. W. Ludwig, Phys. Rev. Lett. **98**, 156802 (2007); arXiv:cond-mat/0609161.
[27] H. E. Castillo, C. C. Chamon, E. Fradkin, P. M. Goldbart, and C. Mudry, Phys. Rev. B **56**, 10668 (1997); arXiv:cond-mat/9706084.
[28] J.-S. Caux, Phys. Rev. Lett. **81**, 4196 (1998); arXiv:cond-mat/9804133.
[29] F. Evers, A. Mildenberger, and A. D. Mirlin, Phys. Rev. B **67**, 041303(R) (2003).
[30] A. D. Mirlin, F. Evers, and A. Mildenberger, J. Phys. A **36**, 3255 (2003); arXiv:cond-mat/0208451.
[31] K. Binder, in *Phase Transitions and Critical Phenomena*, edited by C. Domb and J. Lebowitz (Academic, New York, 1983), Vol. 8, p. 1.
[32] H. W. Diehl and S. Dietrich, Z. Phys. B: Condens. Matter **42**, 65 (1981).
[33] H. W. Diehl and S. Dietrich, Z. Phys. B: Condens. Matter **43**, 281 (1981).
[34] H. W. Diehl, in *Phase Transitions and Critical Phenomena*, edited by C. Domb and J. Lebowitz (Academic, New York, 1986), Vol. 10.
[35] J. L. Cardy, Nucl. Phys. B **240**, 514 (1984).
[36] A. R. Subramaniam, I. A. Gruzberg, A. W. W. Ludwig, F. Evers, A. Mildenberger, and A. D. Mirlin, Phys. Rev. Lett. **96**, 126802 (2006); arXiv:cond-mat/0512040.
[37] S. A. Trugman, Phys. Rev. B **27**, 7539 (1983).
[38] T. Senthil and M. P. A. Fisher, Phys. Rev. B **60**, 6893 (1999); arXiv:cond-mat/9810238.
[39] J. T. Chalker and P. D. Coddington, J. Phys. C **21**, 2665 (1988).
[40] J. T. Chalker and A. Dohmen, Phys. Rev. Lett. **75**, 4496 (1995); arXiv:cond-mat/9510164, Phys. Rev. Lett..
[41] I. A. Gruzberg, N. Read, and S. Sachdev, Phys. Rev. B **55**, 10593 (1997).
[42] I. A. Gruzberg, N. Read, and A. W. W. Ludwig, Phys. Rev. B **63**, 104422 (2001); arXiv:cond-mat/0007254.
[43] N. Read and A. W. W. Ludwig, Phys. Rev. B **63**, 024404 (2000)
[44] F. Merz and J. T. Chalker, Phys. Rev. B **65**, 054425 (2002); arXiv:cond-mat/0106023.
[45] J. T. Chalker, N. Read, V. Kagalovsky, B. Horovitz, Y. Avishai, and A. W. W. Ludwig, Phys. Rev. B **65**, 012506 (2001); arXiv:cond-mat/0009463.
[46] E. J. Beamond, J. Cardy, and J. T. Chalker, Phys. Rev. B **65**,

214301 (2002); arXiv:cond-mat/0201080.
[47] N. Read (unpublished).
[48] R. J. Baxter, *Exactly Solved Models in Statistical Mechanics* (Academic, New York, 1982).
[49] H. Saleur and B. Duplantier, Phys. Rev. Lett. **58**, 2325 (1987).
[50] N. Read and H. Saleur, Nucl. Phys. B **777**, 316 (2007); arXiv:hep-th/0701117.
[51] P. de Gennes, *Scaling Concepts in Polymer Physics* (Cornell University Press, Ithaca, 1988).
[52] M. Janssen, M. Metzler, and M. R. Zirnbauer, Phys. Rev. B **59**, 15836 (1999); arXiv:cond-mat/9810319.
[53] H. Obuse, A. R. Subramaniam, A. Furusaki, I. A. Gruzberg, and A. W. W. Ludwig, Physica E (Amsterdam) **40**, 1404 (2008); arXiv:0709.1018.
[54] A. Mildenberger, A. R. Subramaniam, R. Narayanan, F. Evers, I. A. Gruzberg, and A. D. Mirlin, Phys. Rev. B **75**, 094204 (2007)
[55] A. R. Subramaniam, I. A. Gruzberg, A. W. W. Ludwig, and A. D. Mirlin (unpublished).
[56] M. Scheunert, W. Nahm, and V. Rittenberg, J. Math. Phys. **18**, 155 (1977).
[57] I. A. Gruzberg, A. W. W. Ludwig, and N. Read (unpublished).